EQUIVALENT STATIC WIND LOADS FOR BUFFETING RESPONSE OF BRIDGES

By Xinzhong Chen[1] and Ahsan Kareem[2]

ABSTRACT: In current design practice, the dynamic wind loads are described in terms of the equivalent static wind loads based on the gust response factor. This approach results in a distribution of the equivalent static loading similar to the mean static wind load distribution, which may not always be a physically meaningful and realistic load description. In this paper, the equivalent static load representation for multimode buffeting response of bridges is formulated in terms of either a weighted combination of modal inertial load components, or the background and resonant load components. The focus of the present study is on the determination of weighting factors of equivalent static load components in which the correlation among modal response components due to structural and aerodynamic coupling effects is taken into consideration. It is noteworthy that the equivalent static load distributions vary for each response component. The proposed approach particularly helps in extracting design loads from full aeroelastic model test results by expressing the dynamic loads in terms of the equivalent static loads. This facilitates in drawing useful design input from full aeroelastic tests, which have been employed mostly for monitoring the response of bridge models at selected locations. A simplified formulation is also presented in a closed form when wind loading information is available and coupling in modal response components is negligible, which can be very attractive for the preliminary design application. Examples are presented to illustrate modeling of the equivalent static loading and to demonstrate its effectiveness in bridge design.

INTRODUCTION

In current wind resistant design practice, the dynamic wind loads are generally represented in terms of equivalent static wind loads expressed as the mean static wind loads multiplied by the gust response factor (GRF). The gust response factor, or gust loading factor, was originally introduced by Davenport (1967) and is defined as the ratio of the maximum expected wind load or response to its corresponding mean value. The GRFs are generally different for different response components and may vary in a wide range, depending on the structure system, the wind load characteristics, and the influence functions related to the response components. This GRF approach does not provide useful information in cases with zero mean load or response.

In contrast to the GRF approach, an equivalent static load representation in terms of background and resonant load distributions leads to a physically meaningful and realistic load description (Davenport 1985; Holmes 1992; Kasperski 1992; Holmes and Kasperski 1996; Irwin 1998; Zhou et al. 2000). The background component of the wind load can be treated as a quasi-static load, and its static load distribution for a specific dynamic response depends on the influence function and the distribution of the external wind load. It can be determined based on the load-response-correlation (LRC) approach (Kasperski 1992; Kasperski and Niemann 1992). The resonant load component follows the distribution of the inertial load and can be expressed in terms of modal inertial loads (Davenport 1985; Irwin 1998; Holmes 1999; King 1999).

For design use, the equivalent static load can be expressed in a separated form in terms of the background component and the resonant components of structural modes. The total response is then calculated by combining the background and resonant responses utilizing the square root of the sum of squares (SRSS) combination approach or the complete quadratic combination (CQC) approach. The application of this approach in combining the section model tests for the equivalent wind loads on bridges has been presented by Davenport and King (1984). Alternatively, the equivalent static load can be provided as a linear combination of its background and resonant components using a set of load weighting factors (Irwin 1998; Holmes 1999; King 1999). The resulting structural response can be estimated by means of a static analysis. Such a format facilitates the combination of wind load with other loads and is more appropriate for current design procedures. Instead of using arbitrarily selected load weighting factors (Irwin 1998), a numerical iteration scheme for calculating these weighting factors has been used in King (1999). A methodology based on the LRC approach has been given by Holmes (1999) for the resonant equivalent static load associated with multimode response of bridges without modal response correlations. Representing dynamic load in terms of equivalent static load is particularly suitable for providing the design loads based on wind tunnel tests. Most wind loading information has been derived from section model tests instead of using full bridge aeroelastic model tests, which are traditionally used as a final confirmation of the performance of important bridges. Using the equivalent static load approach, full bridge aeroelastic model tests can be used to gain useful insight into the description of the wind loads (King 1999). This equivalent static load approach can also be used to aid the wind tunnel tests in predicting the response components not directly measured during the test.

Modal response coupling due to closely spaced frequencies and coupled self-excited wind loads may result in significant modal response correlation. For long span suspension bridges, significant aerodynamic coupling between vertical bending and torsional modes exists at higher wind velocities. Neglecting the contribution of these correlations will result in predictions that underestimate the responses (Chen et al. 2000a).

In this paper, the equivalent static load distribution for the multimode buffeting response of bridges is formulated in terms of either a weighted combination of modal inertial load components or the background and resonant load components. The focus of the present study is on the determination of load weighting factors of equivalent static load components, in which the correlation among modal response components due to structural and aerodynamic coupling effects is taken into consideration. The background load component has been ex-

[1]Postdoct. Res. Assoc., Dept. of Civ. Engrg. and Geological Sci., Univ. of Notre Dame, Notre Dame, IN 46556.

[2]Robert M. Moran Prof. and Chair, Dept. of Civ. Engrg. and Geological Sci., Univ. of Notre Dame, Notre Dame, IN 46556.

pressed based on inertial loads and based on external wind load distribution. A simplified formulation is presented in a closed form when wind loading information is available and coupling in modal response components is negligible. Examples are presented to illustrate the modeling of the equivalent static loading and to demonstrate its effectiveness in bridge design.

METHODOLOGY

The dynamic response of a bridge to turbulent wind excitation can be expressed in terms of the matrix equations below:

$$\mathbf{M\ddot{Y}} + \mathbf{C\dot{Y}} + \mathbf{KY} = \mathbf{F} \tag{1}$$

where $\mathbf{M}$, $\mathbf{C}$, and $\mathbf{K}$ = mass, damping, and stiffness matrices, respectively; $\mathbf{Y}$ = dynamic displacement vector; and $\mathbf{F}$ = external stochastic wind load vector, including turbulence induced buffeting and motion induced self-excited components.

Using the modal coordinates, the dynamic displacement and elastic force vectors can be represented as

$$\mathbf{Y} = \sum_j \mathbf{\Phi}_j q_j \tag{2}$$

$$\mathbf{KY} = \mathbf{K} \sum_j \mathbf{\Phi}_j q_j = \mathbf{M} \sum_j \mathbf{\Phi}_j \omega_j^2 q_j = \sum_j \mathbf{P}_{ej0} q_j \tag{3}$$

where $\omega_j = 2\pi f_j$, $\mathbf{\Phi}_j$, and q_j = frequency, mode shape, and modal coordinate of the jth mode; $\mathbf{P}_{ej0} = \mathbf{M\Phi}_j \omega_j^2$ is the unit jth modal inertial load; and $\mathbf{K\Phi}_j = \omega_j^2 \mathbf{M\Phi}_j$ is the orthogonality relationship.

It can be seen from (3) that the dynamic response can be regarded as the quasi-static response under the inertial load excitation. Thus, once the dynamic displacement response is available, any arbitrary dynamic response of interest $z(x_0, t)$ (e.g., bending moment, shear force, and other member forces) can be calculated through a subsequent static analysis and expressed using its influence function vector $\mathbf{A}$ as

$$z(x_0, t) = \mathbf{A} \sum_j \mathbf{P}_{ej0} q_j = \sum_j \rho_j q_j = \sum_j z_j \tag{4}$$

where $\rho_j = \mathbf{AP}_{ej0}$ is the response under $\mathbf{P}_{ej0}$; and $z_j = \rho_j q_j$ is the jth mode component of response $z(x_0, t)$.

The absolute peak value of $z(x_0, t)$ is then given by the CQC approach as

$$z_{\max} = g\sigma_z = g \left(\sum_j \sum_k \sigma_{z_j} \sigma_{z_k} r_{jk} \right)^{1/2} \tag{5}$$

or by the SRSS approach, as follows, when the modal response correlations are negligible:

$$z_{\max} = g\sigma_z = g \left(\sum_j \sigma_{z_j}^2 \right)^{1/2} \tag{6}$$

where

$$\sigma_{z_j} = \rho_j \sigma_{q_j} = \mathbf{AP}_{ej}; \quad \mathbf{P}_{ej} = \mathbf{P}_{ej0}\sigma_{q_j} \tag{7a,b}$$

$$r_{jk} = r_{kj} = \sigma_{q_{jk}}^2/(\sigma_{q_j}\sigma_{q_k}) \tag{7c}$$

where g = peak factor, generally in the range of 3–4; σ_{q_j} and σ_{z_j} = root-mean-square (RMS) values of q_j and jth modal component of $z(x_0, t)$, i.e., $z_j(x_0, t)$; r_{jk} and $\sigma_{q_{jk}}^2$ = correlation coefficient and covariance between jth and kth modal responses; and $\mathbf{P}_{ej}$ = equivalent static load in the jth mode.

The preceding equations indicate that the prediction of other dynamic response components can be conducted based on the available displacement using subsequent static analysis under the equivalent static load, which can be expressed in terms of modal inertial load in each mode. The response component associated with each mode needs to be combined with the

CQC or SRSS approach for the prediction of the total response.

Alternatively, (5) can be rewritten as follows based on the LRC approach:

$$z_{\max} = g\sigma_z = g \sum_j \sigma_{z_j} \left(\sum_k r_{jk}\sigma_{z_k} \right) \Big/ \sigma_z = g\mathbf{A} \sum_j \mathbf{P}_{ej}W_j \tag{8}$$

where W_j = weighting factor of $\mathbf{P}_{ej}$, given by

$$W_j = \sum_k r_{jk}\sigma_{z_k}/\sigma_z = \sum_k r_{jk}\rho_k \sigma_{q_k}/\sigma_z \tag{9}$$

Accordingly, the equivalent static peak load distribution for $z(x_0, t)$ is given in terms of the following linear combination of $\mathbf{P}_{ej}$ as

$$\mathbf{F}_e = g \sum_j \mathbf{P}_{ej}W_j \tag{10}$$

Consider the three-dimensional multimode coupled buffeting response. The dynamic displacement in the vertical, lateral, and torsional directions—$h(x, t)$, $p(x, t)$, and $\alpha(x, t)$, respectively—are expressed as

$$h(x, t) = \sum_j h_j(x)q_j(t); \quad p(x, t) = \sum_j p_j(x)q_j(t) \tag{11a,b}$$

$$\alpha(x, t) = \sum_j \alpha_j(x)q_j(t) \tag{11c}$$

where $h_j(x)$, $p_j(x)$, and $\alpha_j(x)$ = jth mode shapes in the vertical, lateral, and torsional directions, respectively; and x = spanwise position.

The lift, drag, and pitching moment components of the equivalent static modal load in the jth mode are

$$L_{ej}(x) = m(x)h_j(x)\omega_j^2\sigma_{q_j}; \quad D_{ej}(x) = m(x)p_j(x)\omega_j^2\sigma_{q_j} \tag{12a,b}$$

$$M_{ej}(x) = I(x)\alpha_j(x)\omega_j^2\sigma_{q_j} \tag{12c}$$

where $m(x)$ and $I(x)$ = mass and rotational inertia per unit length, respectively.

The RMS value of jth modal response of $z(x_0, t)$ can be calculated through a static analysis and expressed as

$$\sigma_{z_j} = \int_0^l (\beta_L(x)L_{ej}(x) + \beta_D(x)D_{ej}(x) + \beta_M(x)M_{ej}(x)) \, dx = \rho_j\sigma_{q_j} \tag{13}$$

where $\beta_L(x)$, $\beta_D(x)$ and $\beta_M(x)$ = influence functions; and l = span length.

The total peak response $z_{\max}(x_0, t)$ can also be directly calculated through a static analysis under the following equivalent static load distribution:

$$L_e(x) = g \sum_j L_{ej}(x)W_j; \quad D_e(x) = g \sum_j D_{ej}(x)W_j \tag{14a,b}$$

$$M_e(x) = g \sum_j M_{ej}(x)W_j \tag{14c}$$

It can be illustrated that the weighting factor W_j is the correlation coefficient between jth modal inertial load component $\mathbf{P}_{ej0}q_j(t)$ or its effect $z_j(t)$ and response $z(x_0, t)$. The covariance of z_j and z is

$$\sigma_{zz_j}^2 = \sum_k \sigma_{z_{jk}} = \sum_k \rho_j\rho_k\sigma_{q_j}\sigma_{q_k}r_{jk} = \sum_k \sigma_{z_j}\sigma_{z_k}r_{jk} \tag{15}$$

and the correlation coefficient is given by

$$r_j = \sigma_{zz_j}^2/(\sigma_z\sigma_{z_j}) = \sum_k r_{jk}\sigma_{z_k}/\sigma_z = W_j \tag{16}$$

Assuming z and z_j are jointly Gaussian with zero mean, the joint probability density function is expressed as

$$f(z, z_j) = \frac{1}{2\pi\sigma_z\sigma_{z_j}\sqrt{1 - r_j^2}}$$

$$\cdot \exp\left[-\frac{1}{2(1 - r_j^2)}\left(\frac{z^2}{\sigma_z^2} - 2r_j\frac{zz_j}{\sigma_z\sigma_{z_j}} + \frac{z_j^2}{\sigma_{z_j}^2}\right)\right] \qquad (17)$$

The conditional distribution of z_j when $z = g\sigma_z$ is given as

$$f(z_j|z = g\sigma_z) = \frac{f(z = g\sigma_z, z_j)}{f_z(g\sigma_z)} = \frac{1}{\sqrt{2\pi}\sqrt{1 - r_j^2}\sigma_{z_j}}$$

$$\cdot \exp\left(-\frac{(z_j - gr_j\sigma_{z_j})^2}{2(1 - r_j^2)\sigma_{z_j}^2}\right) \qquad (18)$$

where

$$f_z(g\sigma_z) = \frac{1}{\sqrt{2\pi}\sigma_z}\exp\left(-\frac{g^2}{2}\right) \qquad (19)$$

It is clear that $z_j = gr_j\sigma_{z_j} = g\mathbf{A}\mathbf{P}_{ej}W_j$ is the most probable value of z_j when $z = g\sigma_z$. Therefore, the equivalent load $g\mathbf{P}_{ej}W_j$ provides the most probable peak load distribution of the jth modal inertial load for peak response $z = g\sigma_z$. The weighting factors, and hence the equivalent static load distribution, depend on the influence function of the specific response. Therefore, the equivalent static load distributions are unique for each response consisting of multimode contributions. It is also worth noting that only the relative value of the influence function is needed for determining these weighting factors. It is emphasized that, when the response consists of only one mode, the equivalent static load will not depend on the influence function (Holmes 1999). It is same for all response components.

The modal response components and their correlation can be directly quantified through a full aeroelastic model test based on the experimental records of the dynamic displacement, acceleration, bending moment, or other member forces at different locations of the bridge model. When the load information, such as the mean static wind load coefficients, flutter derivatives, admittance function, and the spanwise correlations, are available from section model tests or taut strip model tests, analytical approaches can be utilized for the calculation of dynamic response and associated equivalent static wind load distribution. For long span bridges, multimode coupled analytical approaches can be utilized for the accurate estimate of response including structural and aerodynamic coupling effects (e.g., Katsuchi 1999; Chen et al. 2000a,b).

It is noted that separating the response and corresponding wind load into background and resonant components is not a necessary step for the evaluation of the equivalent static load distribution. However, it is computationally more efficient to calculate the background response by quasi-static analysis directly based on the external wind load distribution rather than by the modal synthesis approach, in which a relatively larger number of modes are required than that for the resonant response analysis. By assuming that the self-excited forces induced by the background response are negligible, the background response, the absolute peak value, and the corresponding equivalent static load distribution are given (Kasperski 1992) by

$$z_b(x_0, t) = \mathbf{A}\mathbf{F}_b \qquad (20)$$

$$z_{b\max} = g\sigma_{z_b} = g\mathbf{A}\mathbf{R}_b\mathbf{A}^T/\sigma_{z_b} \qquad (21)$$

$$\mathbf{P}_{eb} = \mathbf{R}_b\mathbf{A}^T/\sigma_{z_b} \qquad (22)$$

where $\mathbf{F}_b$ = background component of $\mathbf{F}$. It is noted that $\mathbf{P}_{eb}$ can be further expressed in terms of the contributions of the loading modes (Holmes 1992; Chen and Kareem 2000).

The resonant response and modal inertial loads can be given using modal analysis, as mentioned earlier. The total absolute peak value of response is then given by

$$z_{\max} = g\sigma_z = g\sqrt{\sigma_{z_b}^2 + \sigma_{z_r}^2} = g\left(\sigma_{z_b}W_b + \sum_j \sigma_{z_{jr}}W_{jr}\right)$$

$$= g\mathbf{A}\left(\mathbf{P}_{eb}W_b + \sum_j \mathbf{P}_{ejr}W_{jr}\right) \qquad (23)$$

where σ_{z_r} = RMS value of the resonant response z_r; $\sigma_{z_{jr}}$ and $\mathbf{P}_{ejr}$ = RMS value of jth modal resonant response and corresponding inertial load; and W_b and W_{jr} = weighting factors given by

$$W_b = \sigma_{z_b}/\sigma_z; \quad W_{jr} = \sum_k r_{jk}\sigma_{z_{kr}}/\sigma_z \qquad (24a,b)$$

Accordingly, the equivalent static peak load distribution is then given as

$$\mathbf{F}_e = g\left(\mathbf{P}_{eb}W_j + \sum_j \mathbf{P}_{ejr}W_{jr}\right) \qquad (25)$$

It can be illustrated that these weighting factors are the correlation coefficients of corresponding loads or effects with response $z(x_0, t)$.

Using the inertial load distribution corresponding to total modal response including background and resonant components results in a different load distribution for background response compared to that derived from external loads. The former follows the inertial load distribution associated with background response and is more convenient to be applied when structural response can be directly observed, whereas the latter [(22)] depends on the distribution of the external wind load and the influence function, and is more conveniently applied when wind loading information is available. As mentioned earlier, the equivalent static load distribution is not unique; the two representations given here have more physical meaning than that based on the GRF approach.

SIMPLIFIED EXPRESSIONS FOR UNCORRELATED MULTIMODE RESPONSES

Consider the multimode buffeting response of bridges in which the correlations of modal response components are negligible. The mean static, self-excited, and buffeting loads per unit length—i.e., lift (downward), drag (downwind), and pitching moment (nose-up)—are given (Scanlan 1978a,b, 1994; Katsuchi et al. 1999; Chen et al. 2000a) as

$$L_s(x) = -\frac{1}{2}\rho U^2 BC_L; \quad D_s(x) = \frac{1}{2}\rho U^2 BC_D \qquad (26a,b)$$

$$L_s(x) = \frac{1}{2}\rho U^2 B^2 C_M \qquad (26c)$$

$$L_{se}(x, t) = \frac{1}{2}\rho U^2(2b)\left(kH_1^*(k)\frac{\dot{h}}{U} + kH_2^*(k)\frac{b\dot{\alpha}}{U} + k^2 H_3^*(k)\alpha\right.$$

$$\left. + k^2 H_4^*(k)\frac{h}{b} + kH_5^*(k)\frac{\dot{p}}{U} + k^2 H_6^*(k)\frac{p}{b}\right) \qquad (27)$$

$$D_{se}(x, t) = \frac{1}{2}\rho U^2(2b)\left(kP_1^*(k)\frac{\dot{p}}{U} + kP_2^*(k)\frac{b\dot{\alpha}}{U} + k^2 P_3^*(k)\alpha\right.$$

$$\left. + k^2 P_4^*(k)\frac{p}{b} + kP_5^*(k)\frac{\dot{h}}{U} + k^2 P_6^*(k)\frac{h}{b}\right) \qquad (28)$$

$$M_{se}(x, t) = \frac{1}{2} \rho U^2 (2b^2) \left(kA_1^*(k) \frac{\dot{h}}{U} + kA_2^*(k) \frac{b\dot{\alpha}}{U} + k^2 A_3^*(k)\alpha \right.$$

$$\left. + k^2 A_4^*(k) \frac{h}{b} + kA_5^*(k) \frac{\dot{p}}{U} + k^2 A_6^*(k) \frac{p}{b} \right) \tag{29}$$

$$L_b(x, t) = -\frac{1}{2} \rho U^2 B \left(2C_L \chi_{L_{bu}}(k) \frac{u(t)}{U} + (C_L' + C_D)\chi_{L_{bw}}(k) \frac{w(t)}{U} \right) \tag{30}$$

$$D_b(x, t) = \frac{1}{2} \rho U^2 B \left(2C_D \chi_{D_{bu}}(k) \frac{u(t)}{U} + (C_D' - C_L)\chi_{D_{bw}}(k) \frac{w(t)}{U} \right) \tag{31}$$

$$M_b(x, t) = \frac{1}{2} \rho U^2 B^2 \left(2C_M \chi_{M_{bu}}(k) \frac{u(t)}{U} + C_M' \chi_{M_{bw}}(k) \frac{w(t)}{U} \right) \tag{32}$$

where ρ = air density; U = mean wind velocity; $B = 2b$ is the bridge deck width; $k = \omega b/U$ is the reduced frequency; ω = frequency of motion; C_L, C_D, and C_M = static force coefficients, $C_L' = dC_L/d\alpha$, $C_D' = dC_D/d\alpha$, $C_M' = dC_M/d\alpha$; H_j^*, P_j^*, and A_j^* ($j = 1, 2, \ldots, 6$) = flutter derivatives; $\chi_{L_{bu}}$, $\chi_{L_{bw}}$, $\chi_{D_{bu}}$, $\chi_{D_{bw}}$, $\chi_{M_{bu}}$, and $\chi_{M_{bw}}$ = aerodynamic admittance functions; u and w = longitudinal and vertical wind fluctuations; and subscripts s, se, and b designate the static, self-excited, and buffeting components, respectively.

Neglecting the cross-spectral density between the wind fluctuations in the u and w directions, the background modal response is expressed as

$$\sigma_{q_{jb}}^2 = \frac{(0.5\rho UBl)^2}{m_j^2 (2\pi f_j)^4} \int_0^\infty \left(|J_{ju}(f)|^2 S_u(f) + |J_{jw}(f)|^2 S_w(f) \right) df \tag{33}$$

where

$$|J_{ju, jw}(f)|^2 = \frac{1}{l^2} \int_0^l \int_0^l p_{ju, jw}(x_1, k) p_{ju, jw}^*(x_2, k) \mathrm{coh}_{u,w}(x_1, x_2, f) \, dx_1 \, dx_2 \tag{34}$$

$$p_{ju}(x, k) = 2C_L \chi_{L_{bu}}(k) h_j(x) + 2C_D \chi_{D_{bu}}(k) p_j(x) + 2BC_M \chi_{M_{bu}}(k)\alpha_j(x) \tag{35}$$

$$p_{jw}(x, k) = (C_L' + C_D)\chi_{L_{bw}}(k) h_j(x) + (C_D' - C_L)\chi_{D_{bw}}(k) p_j(x)$$
$$+ BC_M' \chi_{M_{bw}}(k)\alpha_j(x) \tag{36}$$

$$\mathrm{coh}_u(x_1, x_2, f) = S_u(x_1, x_2, f)/S_u(f) \tag{37a}$$

$$\mathrm{coh}_w(x_1, x_2, f) = S_w(x_1, x_2, f)/S_w(f) \tag{37b}$$

where l = bridge length; and an asterisk denotes the complex conjugate operator.

The resonant modal response can be expressed as follows by replacing buffeting load as white noise with a constant spectral density at the effective modal frequency:

$$\sigma_{q_{jr}}^2 = \frac{\pi \bar{f}_j (0.5\rho UBl)^2}{4m_j^2 (2\pi \bar{f}_j)^4 \bar{\xi}_j} \left(|J_{ju}(\bar{f}_j)|^2 S_u(\bar{f}_j) + |J_{jw}(\bar{f}_j)|^2 S_w(\bar{f}_j) \right) \tag{38}$$

where the effective frequency $\bar{f}_j$ and damping ratio $\bar{\xi}_j$ are given by

$$\bar{\omega}_j^2 = \omega_j^2 - \frac{\rho b^2 \bar{\omega}_j^2}{m_j} \left(G_{h_j h_j}^{H_4^*}(\bar{k}_j) + G_{h_j p_j}^{H_6^*}(\bar{k}_j) + bG_{h_j \alpha_j}^{H_3^*}(\bar{k}_j) + G_{p_j h_j}^{P_6^*}(\bar{k}_j) \right.$$

$$\left. + G_{p_j p_j}^{P_4^*}(\bar{k}_j) + bG_{p_j \alpha_j}^{P_3^*}(\bar{k}) + bG_{\alpha_j h_j}^{A_4^*}(\bar{k}) + bG_{\alpha_j p_j}^{A_6^*}(\bar{k}) + b^2 G_{\alpha_j \alpha_j}^{A_3^*}(\bar{k}) \right) \tag{39}$$

$$\bar{\xi}_j = \frac{\xi_j \omega_j}{\bar{\omega}_j} - \frac{\rho b^2}{2m_j} \left(G_{h_j h_j}^{H_1^*}(\bar{k}_j) + G_{h_j p_j}^{H_5^*}(\bar{k}_j) + bG_{h_i \alpha_j}^{H_2^*}(\bar{k}_j) + G_{p_i h_j}^{P_5^*}(\bar{k}_j) \right.$$

$$\left. + G_{p_j p_j}^{P_1^*}(\bar{k}_j) + bG_{p_i \alpha_j}^{P_2^*}(\bar{k}_j) + bG_{\alpha_i h_j}^{A_1^*}(\bar{k}_j) + bG_{\alpha_j p_j}^{A_5^*}(\bar{k}_j) + b^2 G_{\alpha_i \alpha_j}^{A_2^*}(\bar{k}_j) \right) \tag{40}$$

where $\bar{k}_j = \bar{\omega}_j b/U = 2\pi \bar{f}_j b/U$; ξ_j = structural damping ratio in the jth mode; and the G terms are defined by the following integral:

$$G_{r_j s_j}^{T_p^*}(\bar{k}_j) = \int_0^l T_p^*(x, \bar{k}_j) r_j(x) s_j(x) \, dx \tag{41}$$

where $T_p^* = H_p^*, P_p^*, A_p^*$ ($p = 1, 2, \ldots, 6$); and $r_j, s_j = h_j, p_j, \alpha_j$.

The background response can also be directly calculated based on the external wind load as

$$\sigma_{z_b}^2(x_0) = (0.5\rho UBl)^2 \int_0^\infty \left(|J_u(f)|^2 S_u(f) + |J_w(f)|^2 S_w(f) \right) df \tag{42}$$

where

$$|J_{u,w}(f)|^2 = \frac{1}{l^2} \int_0^l \int_0^l p_{u,w}(x_1, k) p_{u,w}^*(x_2, k) \mathrm{coh}_{u,w}(x_1, x_2, f) \, dx_1 \, dx_2 \tag{43}$$

$$p_u(x, k) = 2C_L \chi_{L_{bu}}(k)\beta_L(x) + 2C_D \chi_{D_{bu}}(k)\beta_D(x) + 2BC_M \chi_{M_{bu}}(k)\beta_M(x) \tag{44}$$

TABLE 1. Modal Damping Ratio and RMS Buffeting Response of Simply Supported Beam ($L = 200$ m)

Mode number	Damping $\xi_{js} + \xi_{jd}$	Modal Displacement (m) Background	Resonant	Bending Moment ($L/2$) (kgf·m) Background	Resonant	Shear Force ($L/4$) (kgf) Background	Resonant
1	0.0251	0.0238	0.0332	$1.2564e{+}06$	$1.7540e{+}06$	$1.3955e{+}04$	$1.9482e{+}04$
2	0.0087	0.0008	0.0006	0	0	0	0
3	0.0056	0.0001	0.0001	$0.0649e{+}06$	$0.0266e{+}06$	$0.2164e{+}04$	$0.0886e{+}04$
4	0.0046	0	0	0	0	$0.1668e{+}04$	$0.0528e{+}04$
		SRSS		$1.2581e{+}06$ ($1.2344e{+}06$)	$1.7542e{+}06$	$1.4220e{+}04$ ($1.2950e{+}04$)	$1.9510e{+}04$

Note: ( ) indicates result directly calculated based on external load.

TABLE 2. Modal Damping Ratio and RMS Buffeting Response of Simply Supported Beam ($L = 800$ m)

Mode number	Damping $\xi_{js} + \xi_{jd}$	Modal Displacement (m) Background	Resonant	Bending Moment ($L/2$) (kgf·m) Background	Resonant	Shear Force ($L/4$) (kgf) Background	Resonant
1	0.0348	0.0428	0.0681	$1.3987e{+}07$	$2.2252e{+}07$	$3.8839e{+}04$	$6.1790e{+}04$
2	0.0111	0.0019	0.0016	0	0	0	0
3	0.0067	0.0003	0.0002	$0.0959e{+}07$	$0.0488e{+}07$	$0.7992e{+}04$	$0.4061e{+}04$
4	0.0052	0.0001	0	0	0	$0.7089e{+}04$	$0.2832e{+}04$
		SRSS		$1.4020e{+}07$ ($1.3851e{+}07$)	$2.2258e{+}07$	$4.0282e{+}04$ ($3.8112e{+}04$)	$6.1988e{+}04$

Note: ( ) indicates result directly calculated based on external load.
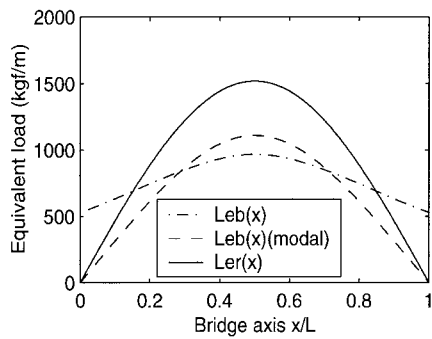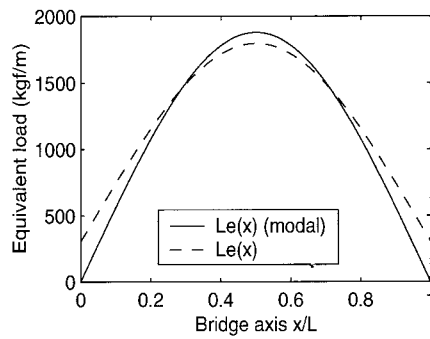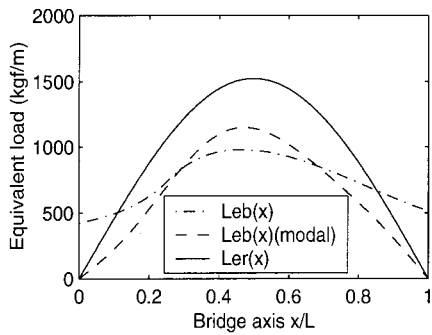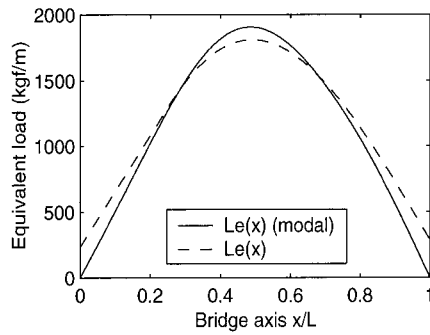
FIG. 1. Equivalent Static Load Distributions for Simply Supported Beam ($L = 200$ m): (a) Background and Resonant Component [Bending Moment ($L/2$)]; (b) Total [Bending Moment ($L/2$)]; (c) Background and Resonant Component [Shear Force ($L/2$)]; (d) Total [Shear Force ($L/2$)]
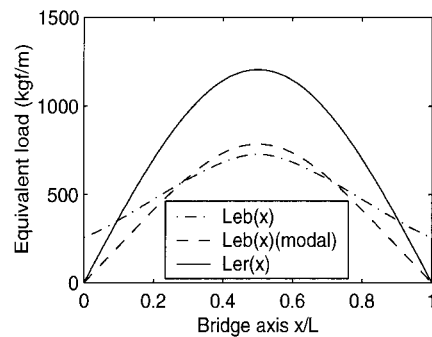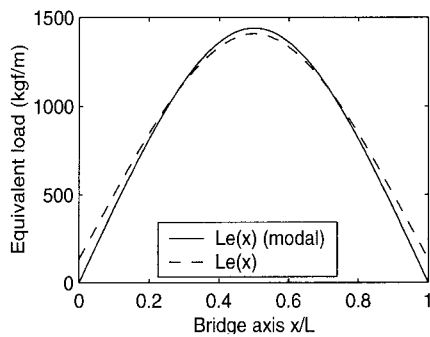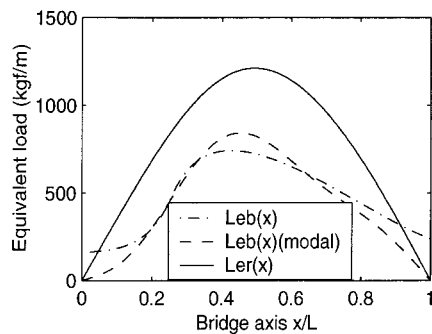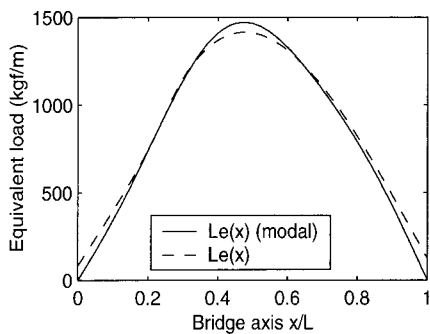
FIG. 2. Equivalent Static Load Distributions for Simply Supported Beam ($L = 800$ m): (a) Background and Resonant Component [Bending Moment ($L/2$)]; (b) Total [Bending Moment ($L/2$)]; (c) Background and Resonant Component [Shear Force ($L/2$)]; (d) Total [Shear Force ($L/2$)]

$$p_w(x, k) = (C'_L + C_D)\chi_{L_{bw}}(k)\beta_L(x) + (C'_D - C_L)\chi_{D_{bw}}(k)\beta_D(x)$$
$$+ BC'_M\chi_{M_{bw}}(k)\beta_M(x) \tag{45}$$

The lift component of the background equivalent static loads is then given by

$$L_{eb}(x) = \frac{(0.5\rho UB)^2}{\sigma_{z_b}} \int_0^\infty \int_0^l ((2C_L)\chi_{L_{bu}}(f)p_u^*(x_1, f)\text{coh}_u(x, x_1, f)S_u(f)$$
$$+ (C'_L + C_D)\chi_{L_{bw}}(f)p_w^*(x_1, f)\text{coh}_w(x, x_1, f)S_w(f)) \, dx_1 \, df \tag{46}$$

with analogous formulations for $D_{eb}(x)$ and $M_{eb}(x)$.

The equivalent static peak loads for $z(x_0, t)$ are given by

$$L_e(x) = g\left(L_{eb}(x)W_b + \sum_j L_{erj}(x)W_{jr}\right) \tag{47a}$$

$$D_e(x) = g\left(D_{eb}(x)W_b + \sum_j D_{erj}(x)W_{jr}\right) \tag{47b}$$

$$M_e(x) = g\left(M_{eb}(x)W_b + \sum_j M_{erj}(x)W_{jr}\right) \tag{47c}$$

To simplify the notation, we will consider the buffeting response in the along-wind direction and only consider the drag induced by the longitudinal wind fluctuations, which is normally dominant. In addition, it is assumed that the coupling among modal response is negligible.
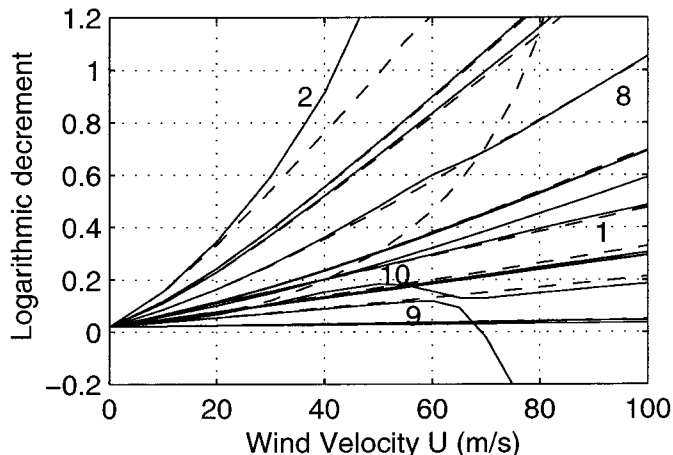
FIG. 3. Damping Ratio versus Wind Velocity (— = with Coupling; −− = without Coupling; Numbers Indicate Modes)
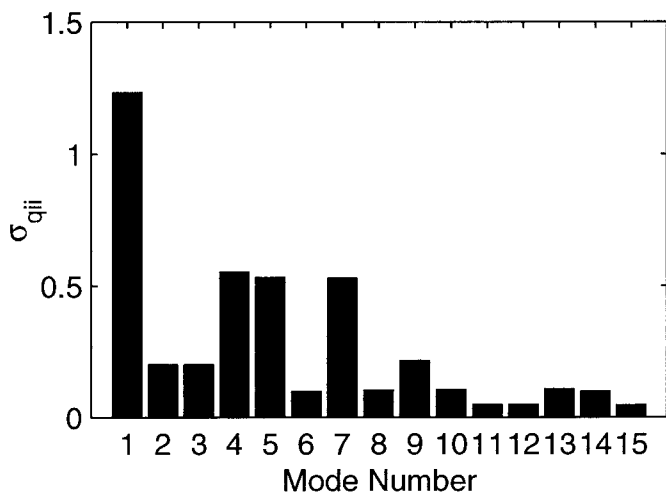
FIG. 4. RMS Modal Displacements ($U = 60$ m/s)

The RMS modal responses and the corresponding equivalent static modal loads are

$$\sigma_{q_{jb},q_{jr}} = \left(\frac{1}{2}\rho U^2 Bl\right)(2C_D)\left(\frac{\sigma_u}{U}\right)\bar{\sigma}_{q_{jb},q_{jr}} \tag{48}$$

$$D_{ejb,ejr}(x) = m(x)\left(\frac{1}{2}\rho U^2 Bl\right)(2C_D)\left(\frac{\sigma_u}{U}\right)\omega_j^2 p_j(x)\bar{\sigma}_{q_{jb},q_{jbr}} \tag{49}$$

where

$$\bar{\sigma}_{q_{jb}}^2 = \int_0^\infty |J_{ju}(f)|^2 |\chi_{Du}(f)|^2 S_u(f)/\sigma_u^2 \, df/(m_j\omega_j^4) \tag{50}$$

$$\bar{\sigma}_{q_{jr}}^2 = \pi f_j |J_{ju}(f_j)|^2 |\chi_{Du}(f_j)|^2 S_u(f_j)/\sigma_u^2/(4m_j^2\omega_j^4(\xi_{js} + \xi_{jd})) \tag{51}$$

$$|J_{ju}(f)|^2 = \frac{1}{l^2} \int_0^l \int_0^l p_j(x_1)p_j(x_2)\text{coh}_u(x_1, x_2, f) \, dx_1 \, dx_2 \tag{52}$$

It is assumed the self-excited forces only change the damping terms by the aerodynamic damping given by the following quasi-steady formula:

$$\xi_{jd} = -\frac{\rho B^2 P_1^*}{8m_j}\int_0^l p_j^2(x) \, dx = \left(\frac{C_D}{4\pi}\right)\left(\frac{\rho B^2}{m_{j0}}\right)\left(\frac{U}{f_j B}\right) \tag{53}$$

where $m_{j0} = m_j/\int_0^l p_j^2(x) \, dx$.

The background RMS value and corresponding equivalent static load distribution for $z(x_0, t)$ is

$$\sigma_{z_b}(x_0) = \left(\frac{1}{2}\rho U^2 Bl\right)(2C_D)\left(\frac{\sigma_u}{U}\right)\bar{\sigma}_{z_b} \tag{54}$$

$$D_{eb}(x) = \left(\frac{1}{2}\rho U^2 B\right)(2C_D)\left(\frac{\sigma_u}{U}\right)$$
$$\cdot \int_0^\infty J_{u0}(x, f)|\chi_{Du}(f)|^2 S_u(f)/\sigma_u^2 \, df/\bar{\sigma}_{z_b} \tag{55}$$

where

$$\bar{\sigma}_{z_b}^2(x_0) = \int_0^\infty |J_u(f)|^2 |\chi_{Du}(f)|^2 S_u(f)/\sigma_u^2 \, df \tag{56}$$

$$|J_u(f)|^2 = \frac{1}{l^2} \int_0^l \int_0^l \beta_D(x_1)\beta_D(x_2)\text{coh}_u(x_1, x_2, f) \, dx_1 \, dx_2 \tag{57}$$

$$J_{u0}(x, \omega) = \frac{1}{l} \int_0^l \beta_D(x_1)\text{coh}_u(x, x_1, f) \, dx_1 \tag{58}$$

Similar expressions for the vertical motion can be written
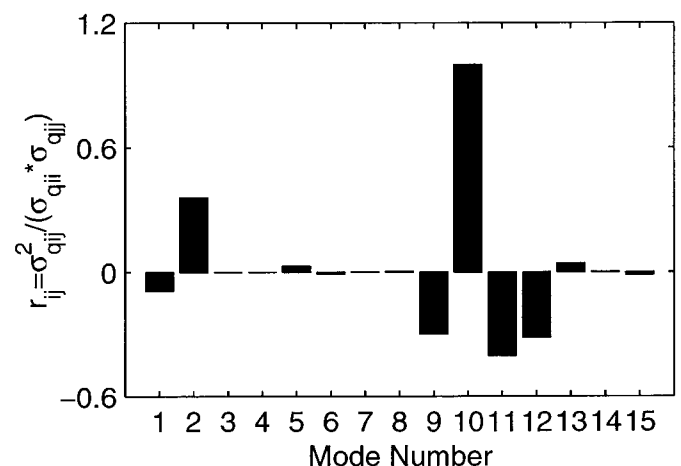
FIG. 5. Correlation Coefficients between Mode 10 and Other Modes ($U = 60$ m/s)

with $(C_L' + C_D)$ replacing $2C_D$ and w replacing u. For the torsion case, B^2 replaces B, C_M' replaces $2C_D$, $I(x)$ replaces $m(x)$, and w replaces u.

NUMERICAL EXAMPLES

Example A: Simply Supported Beams

To illustrate the proposed methodology, the vertical buffeting response of simply supported beams with span lengths of
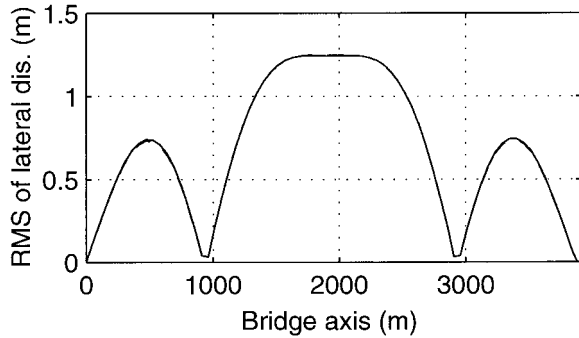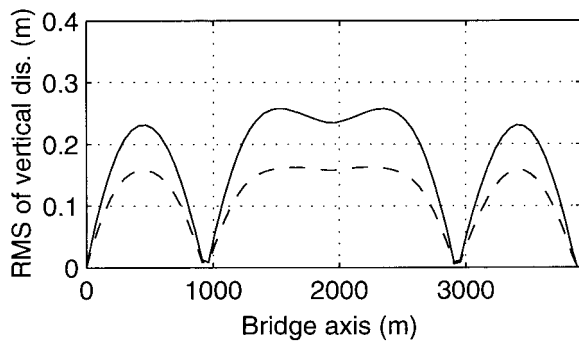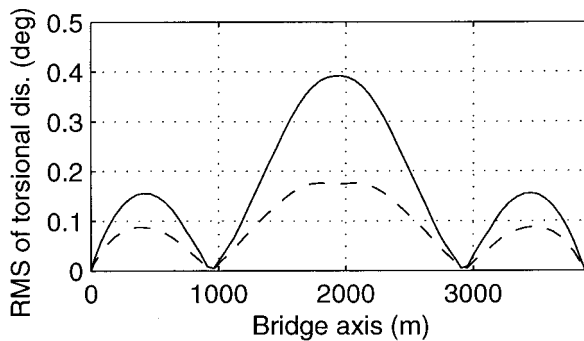
FIG. 6. RMS Responses of Displacement ($U = 60$ m/s; — = with Coupling; –– = without Coupling)

200 and 800 m under vertical wind fluctuation were chosen as examples. The fundamental frequencies and mass per unit length were 0.45 and 0.25 Hz, and 16 and 20 tonne/m, respectively. Other parameters were the same for both examples. The von Karman spectrum with a length scale $L_w^y = 50$ m, intensity $\sigma_w/U = 5\%$, and exponential coherence function with a decay factor 8 were used. The admittance function was calculated using Sears' function and the aerodynamic damping was evaluated using quasi-steady theory. Other parameters were $U = 60$ m/s, $C_L' = 1.5$, $C_D = 0.3$, $B = 20$ m and $g = 3.5$.

The bending moment at the midspan and shear force at the quarter span were considered for the determination of the equivalent static load distributions. The first four modes were considered in the calculation when using the modal synthesis technique and the modal response correlations were assumed to be negligible. The modal logarithmic decrement for each mode was assumed to be 0.02. The background response and corresponding equivalent static load were also calculated based on the external wind load distribution. In the evaluation of the background component, the upper limit of the integrals was chosen as the first natural frequency.

Tables 1 and 2 summarize the results of the modal damping ratios, the generalized modal responses, and the modal components of the moment and shear force for the 200 and 800 m spans, respectively. The equivalent static wind load distributions are shown in Figs. 1 and 2.

The background load distributions were calculated from both inertial load and external load. These result in different distributions, but both gave almost the same response. While the load distributions based on the inertial load result in a zero loading at the ends of the beam by the mode shapes, the load distributions based on the external wind load do not necessarily follow this constraint at these boundary locations. The background component decreased with the increase in span length. The ratios between the background and resonant components depend on the external wind load and dynamic characteristics of the beam. For very long span bridges the resonant component is generally dominant, but the background component should be carefully taken into account for bridges with medium and shorter spans. In both examples, the fundamental modal response is dominant; thus, the equivalent load distributions for moment and shear force have similar distributions.

Example B: Long Span Suspension Bridge

A long span suspension bridge with a main span of approximately 2,000 m was considered as an example to illustrate the methodology proposed in this paper. In this example, the buffeting response of displacement to turbulent wind excitation was calculated based on a three-dimensional multimode coupled buffeting analysis approach conducted in the frequency domain. Fifteen lower natural modes with frequencies ranging between 0.03 and 0.2 Hz are included in the analysis. Detailed discussions and descriptions of the analytical ap-

TABLE 3. Weighting Factors for Equivalent Static Modal Loads (with Coupling)

Response	Mode 1	Mode 2	Mode 3	Mode 4	Mode 6	Mode 8	Mode 9	Mode 10
V-D ($L/2$)	—	0.892	—	—	—	0.549	—	—
V-BM ($L/2$)	—	0.256	—	—	—	0.926	—	—
V-D ($L/4$)	—	0.441	0.798	—	0.328	0.296	—	—
V-BM ($L/4$)	—	0.125	0.713	—	0.299	0.605	—	—
L-D ($L/2$)	0.993	—	—	—	—	—	0.122	—
L-BM ($L/2$)	0.641	—	—	—	—	—	0.763	−0.179
L-D ($L/4$)	0.845	—	—	0.506	—	—	0.179	−0.120
L-BM ($L/4$)	0.302	—	—	0.799	—	—	0.509	−0.128
T-D ($L/2$)	0.192	—	—	—	—	—	−0.065	0.931
T-D ($L/4$)	—	—	—	0.440	—	—	−0.134	0.876

Note: L, V, and T = lateral, vertical, and torsional; D and BM = displacement and bending moment.

TABLE 4. Weighting Factors for Equivalent Static Modal Loads (without Coupling)

Response	Mode 1	Mode 2	Mode 3	Mode 4	Mode 6	Mode 8	Mode 9	Mode 10
V-D ($L/2$)	—	0.865	—	—	—	0.484	—	—
V-BM ($L/2$)	—	0.205	—	—	—	0.902	—	—
V-D ($L/4$)	—	0.490	0.644	—	0.474	0.280	—	—
V-BM ($L/4$)	—	0.116	0.546	—	0.404	0.663	—	—
L-D ($L/2$)	0.991	—	—	—	—	—	0.135	—
L-BM ($L/2$)	0.593	—	—	—	—	—	0.881	0.229
L-D ($L/4$)	0.846	—	—	0.499	—	—	0.183	—
L-BM ($L/4$)	0.292	—	—	0.771	—	—	0.556	0.153
T-D ($L/2$)	0.434	—	—	—	—	—	0.600	0.775
T-D ($L/4$)	0.160	—	—	0.686	—	—	0.395	0.649

Note: L, V, and T = lateral, vertical, and torsional; D and BM = displacement and bending moment.
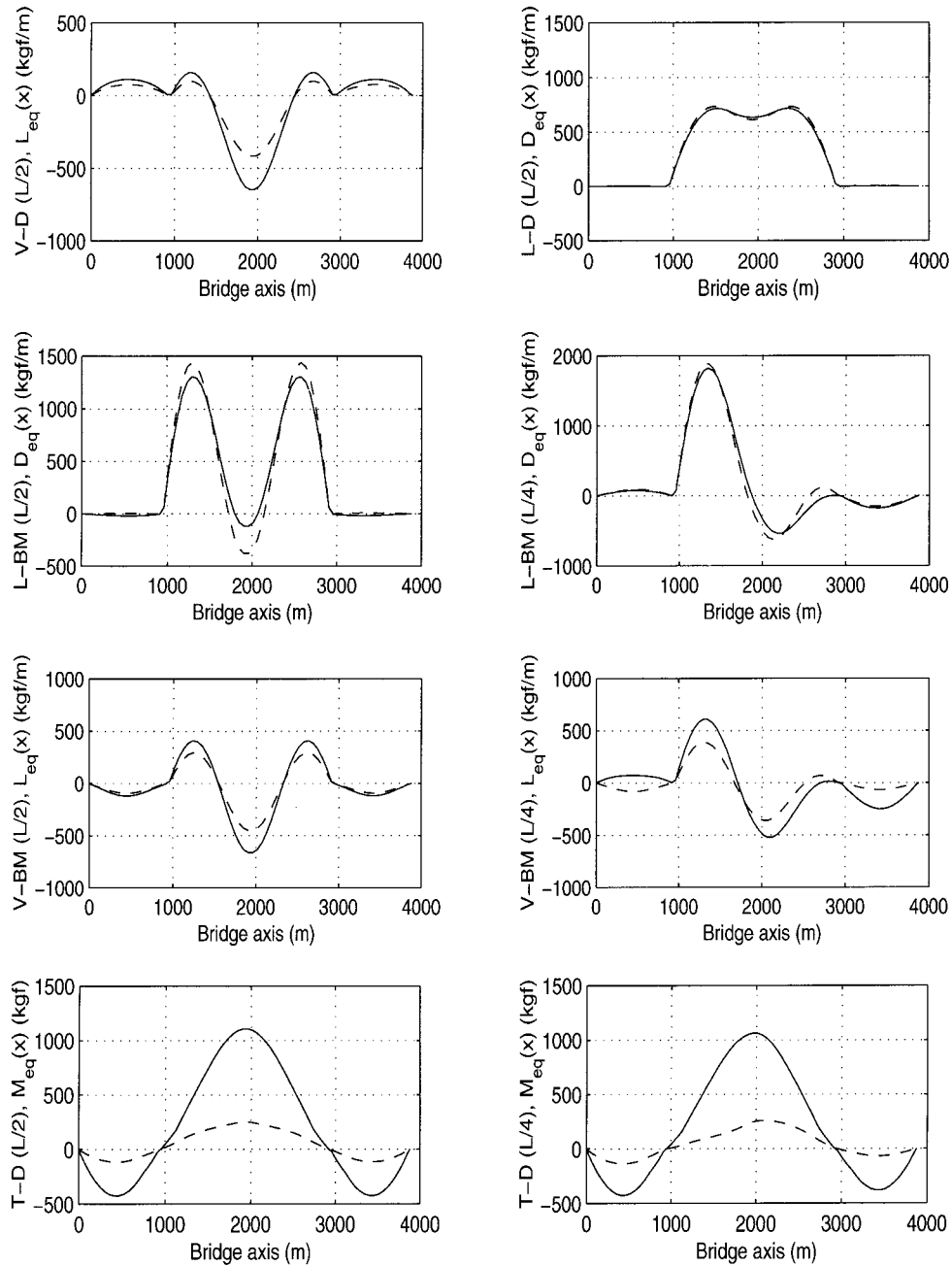
FIG. 7. Equivalent Static Load Distribution for Different Wind Effects (U = 60 m/s; — = with Coupling; – – = without Coupling)

proach and the parameters used can be found in Chen et al. (2000a).

Fig. 3 shows the changes in damping ratio with the mean wind velocity, which includes both the structural and aerodynamic damping. The solid lines and dashed lines represent the results with and without aerodynamic coupling effects, calculated using a multimode coupled approach and (40), respectively. Significant changes in the aerodynamic damping can be identified due to the aerodynamic coupling at higher wind velocities. It is noted that the self-excited forces not only influ-

ence the damping ratios but also result in modal coupling particularly between the vertical bending and torsional directions.

Fig. 4 shows the modal displacements in different modes at 60 m/s. Fig. 5 shows the correlation coefficients between modal response components associated with mode 10 and others. Fig. 6 shows the RMS lateral, vertical, and torsional displacements along the bridge axis at 60 m/s. The solid lines and the dashed lines represent, respectively, the result with and without the aerodynamic coupling. This displacement information is the basis for the estimation of the equivalent static load.

Displacements and bending moments in the lateral and vertical directions and the displacement in the torsional direction at the midspan and quarter span of the main span were selected for consideration of the equivalent static loads. Tables 3 and 4 show the weighting factors concerning modal inertial loads, which only include the combination of the important modes. Fig. 7 shows the corresponding absolute equivalent static peak load distributions excluding the mean wind load components. The peak factor was assumed to be 3.5. It is clear that, for different response components, the equivalent static load distributions are different. The accuracy of the calculated static load distributions depends on the accuracy of the relative value of the influence function.

CONCLUSIONS

The methodology for calculating the equivalent static load distribution associated with a given dynamic response component of interest has been presented, which includes the correlation among modal response components. The equivalent static load has been expressed in terms of a weighted combination of modal inertial load components, or the background and resonant components. Using the proposed methodology, the weighting factors can be easily determined instead of relying on an arbitrary selection or a complex estimation procedure. The key advantage of the procedure is in its prediction of design loads for other dynamic response components based on generally available displacement response. It is particularly useful for the representation of design loads based on full aeroelastic model test results, and it meets the current wind design practice. Simplified formulations presented here can be used for preliminary design of bridges.

Applications to simply supported beams and a long span suspension bridge were presented to illustrate the effectiveness of the methodology. The aerodynamic coupling was shown to have significant influence on the equivalent static load distribution for long span bridges. For potential application in design practice, it is necessary to limit the number of distributions to only critical response components and to simplify the mode shapes for a convenient representation of the load distributions.

REFERENCES

Chen, X., and Kareem, A. (2000). ''On the application of stochastic decomposition in the analysis of wind effects.'' *Proc., Int. Conf. on Advances in Struct. Dyn.*, Hong Kong, 135–142.

Chen, X., Matsumoto, M., and Kareem, A. (2000a). ''Aerodynamic coupling effects on flutter and buffeting of bridges.'' *J. Engrg. Mech.*, ASCE, 126(1), 17–26.

Chen, X., Matsumoto, M., and Kareem, A. (2000b). ''Time domain flutter and buffeting response analysis of bridges.'' *J. Engrg. Mech.*, ASCE, 126(1), 7–16.

Davenport, A. G. (1964). ''Note on the distribution of the largest value of a random function with application to gust loading.'' *J. Inst. of Civ. Engrg.*, London, 24, 187–196.

Danenport, A. G. (1967). ''Gust loading factors.'' *J. Struct. Engrg. Div.*, ASCE, 93(1), 11–34.

Davenport, A. G. (1985). ''The representation of the dynamic effects of turbulent wind by equivalent static wind loads.'' *Proc., 1985 Int. Engrg. Symp. on Struct. Steel*, Chicago, 1–13.

Davenport, A. G., and King, J. P. C. (1984). ''Dynamic wind forces on long span bridges.'' *Proc. 12th IABSE Congr.*, International Association of Bridge and Structural Engineers, Zurich.

Holmes, J. D. (1992). ''Optimized peak load distributions.'' *J. Wind Engrg. and Indust. Aerodyn.*, 41–44, 267–276.

Holmes, J. D. (1999). ''Equivalent static load distributions for resonant dynamic response of bridges.'' *Proc., 10th Int. Conf. on Wind Engrg.*, Copenhagen, 907–911.

Holmes, J. D., and Kasperski. (1996). ''Effective distributions of fluctuating and dynamic wind loads.'' *Australian Civ./Struct. Engrg. Trans.*, 38, 83–88.

Irwin, P. A. (1998). ''The role of wind tunnel modeling in the prediction of wind effects on bridges.'' *Bridge aerodynamics*, Balkema, Rotterdam, The Netherlands, 59–85.

Kasperski, M. (1992). ''Extreme wind load distributions for linear and nonlinear design.'' *Engrg. Struct.*, 14, 27–34.

Kasperski, M., and Niemann, H.-J. (1992). ''The LRC (load-response-correlation) method: a general method of estimating unfavorable wind load distributions for linear and nonlinear structural behavior.'' *J. Wind Engrg. and Indust. Aerodyn.*, 43, 1753–1763.

Katsuchi, H., Jones, N. P., and Scanlan, R. H. (1999). ''Multimode coupled flutter and buffeting analysis of the Akashi-Kaikyo Bridge.'' *J. Struct. Engrg.*, ASCE, 125(1), 60–70.

King, J. P. C. (1999). ''Integrating wind tunnel tests of full aeroelastic models into the design of long span bridges.'' *Proc., 10th Int. Conf. on Wind Engrg.*, Copenhagen, 927–934.

Scanlan, R. H. (1978a). ''The action of flexible bridges under wind. I: Flutter theory.'' *J. Sound and Vibration*, 60(2), 187–199.

Scanlan, R. H. (1978b). ''The action of flexible bridges under wind. II: Buffeting theory.'' *J. Sound and Vibration*, 60(2), 201–211.

Scanlan, R. H. (1993). ''Problematic in formulation of wind-force models for bridge decks.'' *J. Engrg. Mech.*, ASCE, 119(7), 1353–1375.

Zhou, Y., Kareem, A., and Gu, M. (2000). ''Equivalent static buffeting loads on structures.'' *J. Struct. Engrg.*, ASCE, 126(8), 989–992.